Int J Clin Exp Med 2018;11(4):3078-3085
www.ijcem.com /ISSN:1940-5901/IJCEM0063223

Original Article

Construction of a three-dimensional interactive digital atlas of the dural sinus and deep veins based on human head magnetic resonance images by a comprehensive modeling protocol

Zhirong Yang, Zhilin Guo

Department of Neurosurgical, The Ninth People Hospital, Medical School, Shanghai Jiaotong University, Shanghai 200011, China

Received August 7, 2017; Accepted January 25, 2018; Epub April 15, 2018; Published April 30, 2018

Abstract: Objectives: To design a three-dimensional (3D) interactive digital atlas of the human dural sinus and deep veins for assisting neurosurgeons in preoperative planning and neurosurgical training. Methods: Sagittal head magnetic resonance (MR) images were obtained of a 54-year-old female who suffered from left posterior fossa tumor. A comprehensive modeling protocol consisting of five steps including thresholding, crop mask, region growing, 3D calculating and 3D editing was used to develop a 3D digital atlas of the dural sinuses and deep veins based on the MR images. The accuracy of the atlas was also evaluated. Results: The 3D digital atlas of the human dural sinus and deep veins was successfully constructed using 176 sagittal head MR images. The contours of the acquired model matched very well with the corresponding structures of the original images in axial and oblique view of MR cross-sections. The atlas can be arbitrarily rotated and viewed from any direction. It can also be zoomed in and out directly using the zoom function. Conclusion: A 3D digital atlas of human dural sinus and deep veins was successfully created, it can be used for repeated observations and research purposes without limitations of time and shortage of corpses. In addition, the atlas can potentially be used for preoperative planning and surgical training.

Keywords: Three-dimensional (3D), human dural sinus, deep veins

Introduction

The dural sinuses form a channel system that functions primarily as collection and drainage of the intracranial venous blood [1]. The deep venous system connects with the straight sinus by the vein of Galen behind the splenium of the corpus callosum. The dural sinuses and deep veins also serve as important landmarks in neurosurgery [2-9], and understanding of their complex anatomical features facilitates preoperative planning and navigation through the neurosurgical landscape. They also gain clinical significance in cases of trauma, meningioma and, though rare, dural sinus thrombosis [10].

However, the spatial structure of the dural sinuses and deep veins cannot be visualized directly by gross observation or head magnetic resonance imaging (MRI). Digital subtraction angiography typically only displays brain structural images in two dimensions and does not yield full configurations of the dural sinuses and deep veins. On the other hand, three dimensional (3D) digital atlases are more effective than two dimensional (2D) methodologies in displaying spatial morphology of the brain [11]. In our earlier study, we constructed a 3D digital dural atlas of the human brain, demonstrated the feasibility of virtually visualizing the dural structures with the digital atlas and provided an interactive queuing tool for surgical training and preoperative planning. Given the unique anatomy and neuroanatomic significance of the dural sinuses and deep veins, in the current study, we further delineated the 3D digital atlas of the dural sinus and deep veins which can be queried interactively.

Table 1. The operating parameters of sinuses and cerebral veins

	Thresholding		Crop mask	Operating		
	Mix	Max	x × y × z, mm^3	Region growing (t)	3D calculate	3D edit
Head MRI	0	2287	-	-	-	-
Block						
A	571	1403	10 × 19.5 × 36	1		
B	696	1342	49 × 62 × 113	1		
C	815	1441	27 × 37 × 106	2		
D	517	1004	51 × 40 × 106	3		Manual
E	855	1750	29 × 41 × 46	1	Optimal	-
Bilateral superior petrosal sinus	477	1024	16 × 47 × 104	2		Manual
Left inferior petrosal sinus	556	2098	25 × 35 × 37	1		Manual
Deep cerebral veins	576	894	31 × 60 × 49	3		Manual

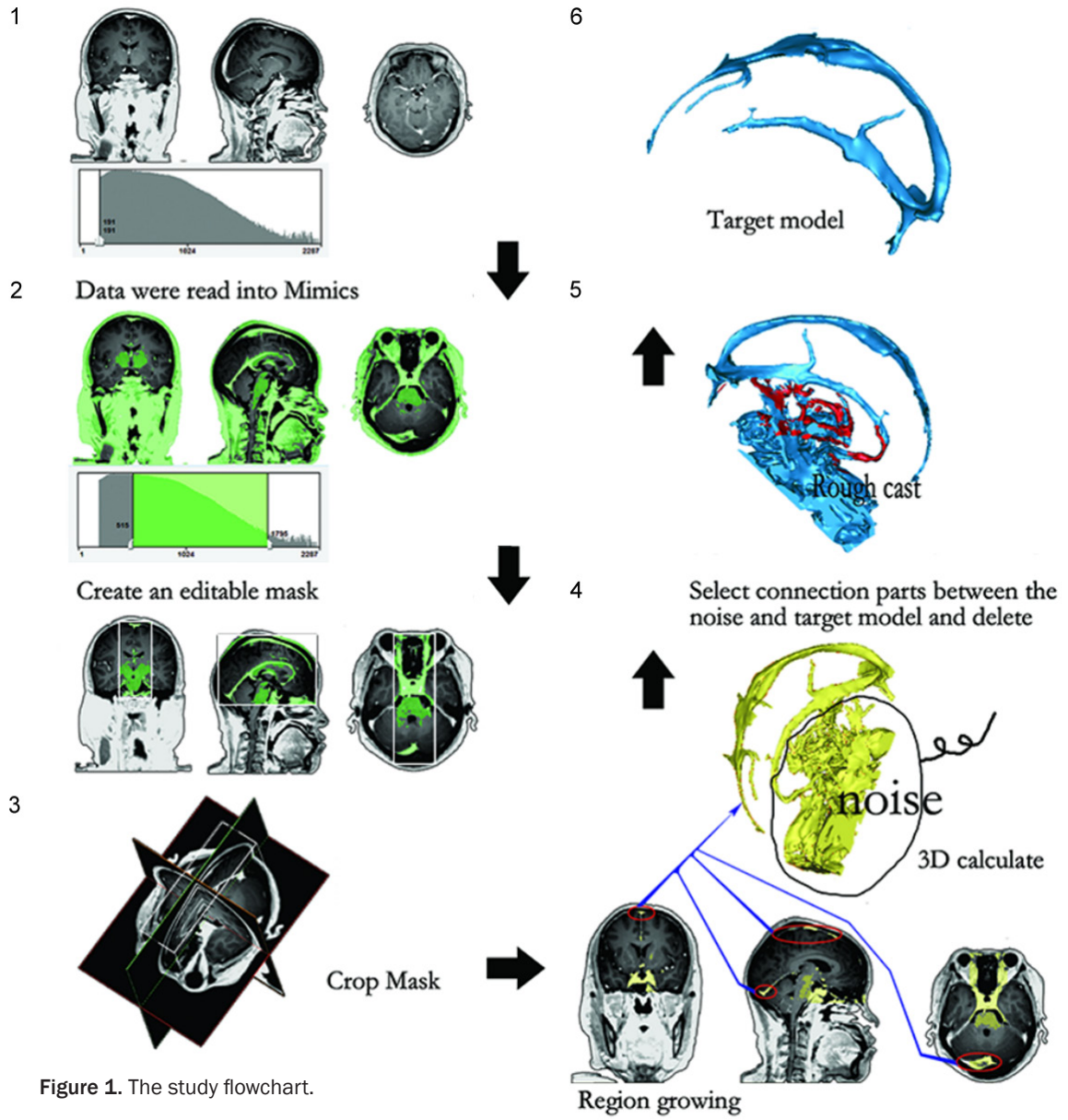

Figure 1. The study flowchart.

Table 2. List of structures based on contrast-enhanced T1 weighted MRI in this paper

Head MRI	176
Masks	9
Substructures	9
Base model	1
Dural sinuses, total images	1
Deep veins, total images	1
PDFs	1

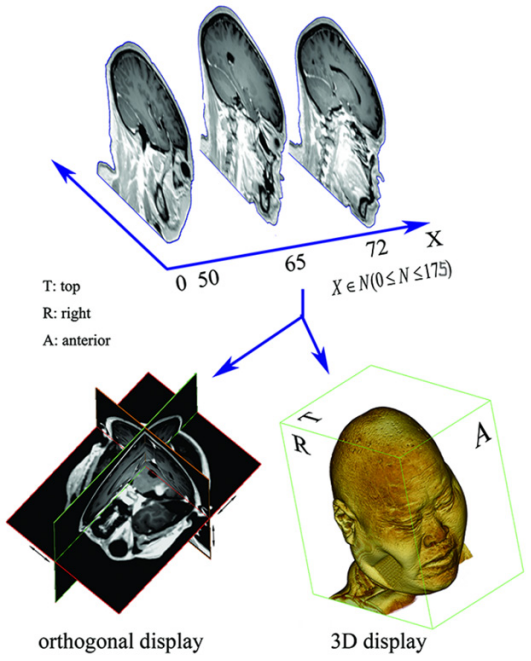

Figure 2. Image organizing sequence, a 3-D data organized by the 176 sagittal images.

Methods

Data acquisition

Sagittal contrast enhanced T1 weighted images were obtained from a 54-year-old female subject with a left posterior fossa tumor. Head MRI scan was performed on 3.0 T with 32 channels and initial pictures of DICOM were taken as the raw data. The parameters used to acquire MRI data were as follows: slice thickness 1.0 mm, interslice gap 1.0 mm, dimensions and field of view 512 × 512 voxels, and total number of layers 176. The dural sinus was segmented into six blocks: block I: the superior and inferior sagittal sinuses, straight sinus; block II: bilateral transversesinuses, and confluence of sinuses; block III: bilateral sigmoid sinuses; block IV: bilateral sphenoparietal sinus; block V: cavernous sinus; block VI: bilateral superiorpetrosal sinus and the left inferior petrosal sinus. The right inferior petrosal sinus was not investigated because it failed to be visualized in head MRI.

Model construction

The thresholding procedure was used to generate masks from original head MRI data. The Mimics software (Materialise's, Belgium) was used, it presented segmentation functions based on image density thresholds. The threshold jail of the image mask fell within the range from 0 to 2287 (**Table 1**). The threshold jail value of 0 was taken as background and the values above 2287 were considered as noises, excluding normal anatomic structures. The block including target structures was segmented from the thresholding mask to obtain block mask. Generated masks were further processed using an embedded region growing algorithm in Mimics and then reconstructed into a 3D model. The surface model was refined automatically and further checked by cross-sectioning the surface models with original head MRI and manually revised using 3ds Max (version 11.0, Autodesk, USA) until it accorded with the correct anatomy. The dural sinus model was outputted in the SLT format and imported into 3-matic viewer for format conversion. The 3D dural sinus model was exported from the 3-matic viewer into Adobe Acrobat 11 Pro (http://www.adobe.com) to create interactive 3D portable document format (PDF) files, which can be displayed and rotated in any directions using any structure as the focal point of rotation.

Model validation

For evaluation of the accuracy of the superior sagittal sinus and inferior sagittal sinus, we imported the 3D dural sinus atlas into the 3D data system of the raw head MRI images, and the 3D dural sinus model was validated by matching the cross-section of the surface models with the original head MRI. Furthermore, a random marker was placed in the 3D dural sinus atlas and the corresponding coordinates of the marker in head MRI images were verified by naked eye. The accuracy of the dural sinus and deep veins was evaluated by separately examining the midline and the skull base struc-

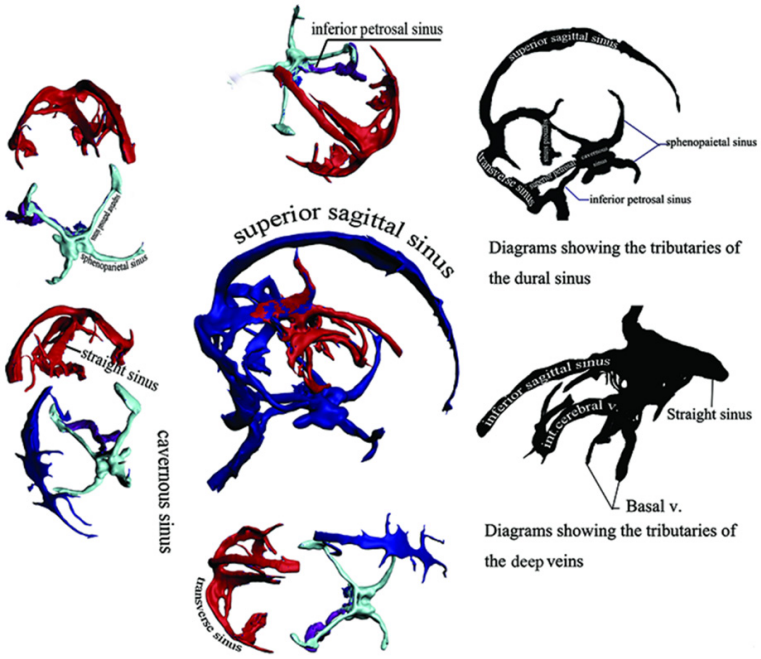

Figure 3. This figure shows the dural sinus and deep veins, surrounded by the decomposition model from various angles.

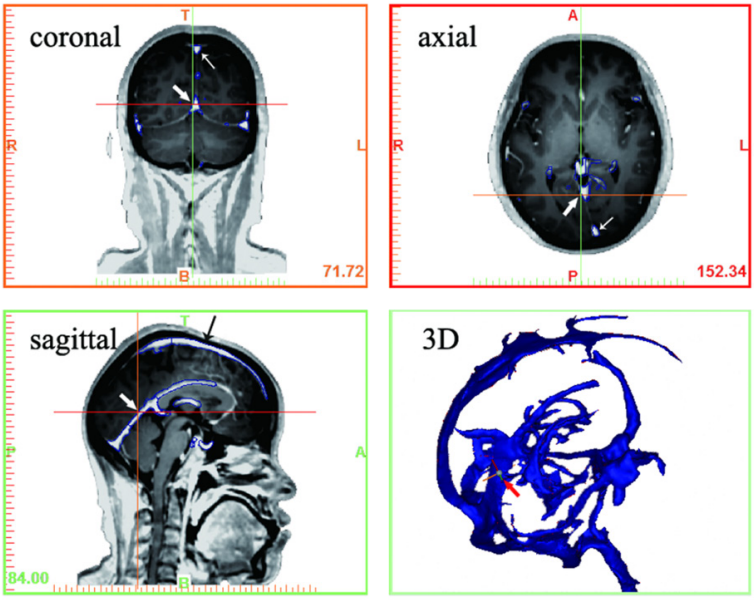

Figure 4. Atlas data in the reference frame displayed in Mimics environment. It shows the contours of the dural sinus and deep veins model match very well on the corresponding structure edge in three orthogonal (axial, coronal and sagittal view) MRI cross-section. The cross line is positioned on the corresponding coordinates of marker point in the three orthogonal slices comprising this point. Clicking in any point within the model will display the three orthogonal slices comprising this point and the automatic adjustment of the corresponding coordinates. Arrows were manually added for indicating marker information but are not displayed by Mimics software.

tures. In addition, for evaluation of the transverse sinus and the superior petrosal vein in the skull base, a reference model was created of the anterior, middle and posterior skull base with head MRI data and a dural mater reference model was also constructed; these models were compared with the dural sinus and deep vein atlas for consistency of contours in the reference model and the atlas. Furthermore, a reference model was established in the 3D Max and the dural sinus model in.stl format was imported into the 3D Max and registered with the reference model for observation. We checked up the accuracy of our 3D dural sinus and deep venous model by cross-sectioning the surface models and matching original head MRI images and by consistency between the placed marker and its corresponding coordinates in the three orthogonal slices in Mimics. The coordinates of the base model was set the same as the original scan coordinate.

Results

The study flowchart is shown in **Figure 1**. We acquired totally 176 head MR sagittal images with a matrix size of 256 × 256 using a 3.0 T MR scanner. All data sets of head MRI, masks, substructures, the base reference model, dural sinus and deep vein panoramic images and their PDF's are listed in **Table 2**. The main dural sinus structure was clearly visualized in most head MRI images. The slice distance was 1.0 mm. These sagittal images were successfully organized into a single 3-D

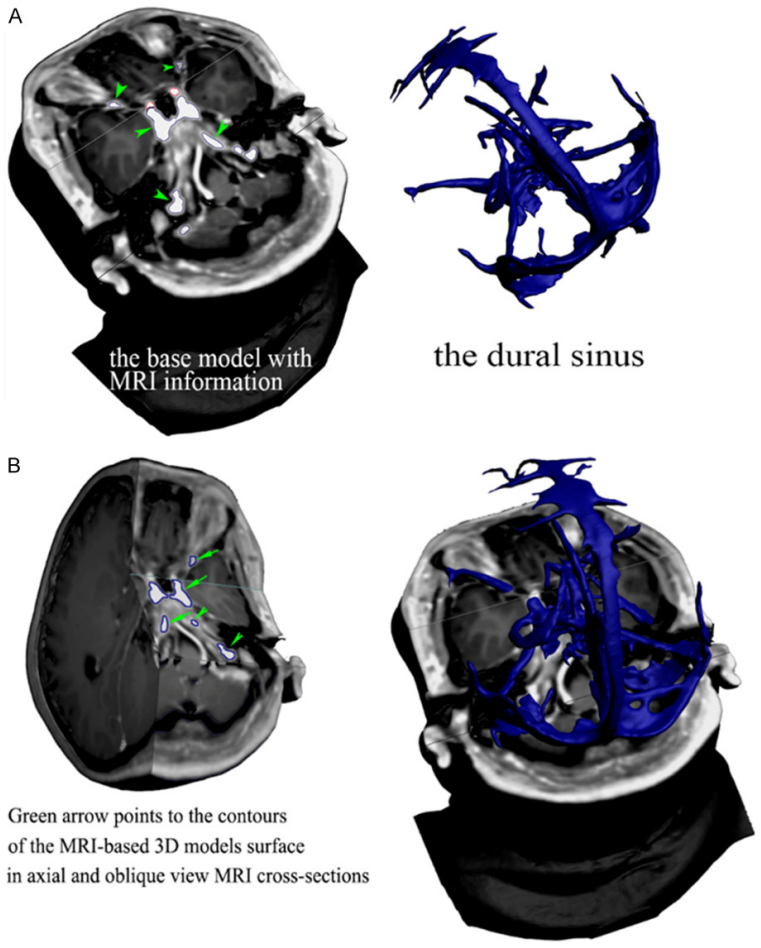

Figure 5. A base model with head MRI information. The five green arrows in left picture indicate the contours of the dural sinus and deep veins model match very well on the corresponding structure edge in axial and oblique view) MRI cross-sections.

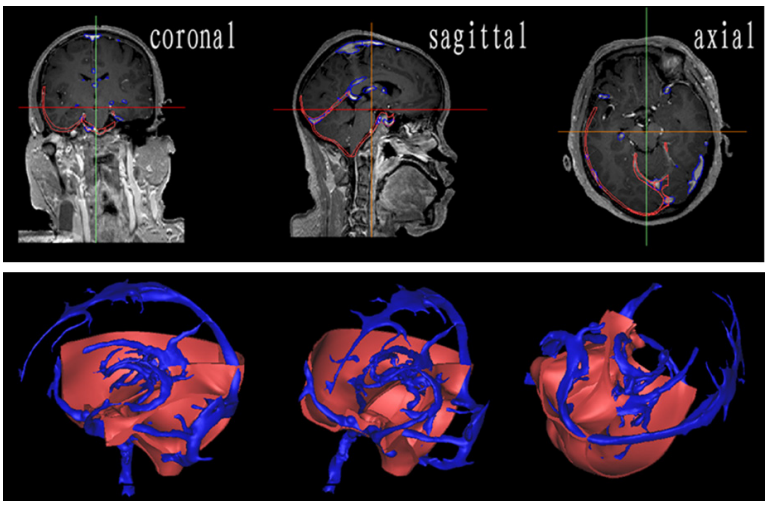

Figure 6. Overview of the 3-D model.

entity (**Figure 2**). The dural sinus and deep vein atlas was created and can be separated from the main cerebral structures and was observable from different angles (**Figure 3**).

The superior sagittal sinus was viewed in the midline area (**Figure 4**). The superior and inferior sagittal sinus contour lines agreed very well with the MRI image edges of the corresponding structure. The coordinates of the random marker placed on the inferior sagittal sinus was automatically created on the front surface and shown as a cross sign (**Figure 4**). The cross-sectional contour of the sphenoparietal sinus, cavernous sinus and superior petrosal sinus matched very well with MRI image edges of the reference model (**Figure 5**). The dural sinus and deep vein were adapted into the corresponding parts in the reference model (**Figure 6**). The contour lines of the venous sinuses, deep veins and the reference model matched very well with their counterparts in the original head MRI images. In the 3D environment, the venous sinuses and deep veins are consistent with the original head data (**Figure 7**).

A surgical incision was made by calculating the venous sinus boundary in advance. The lines were then drawn on the patient's head in order to precisely locate the flap (**Figure 8**). We further compared our 3D model to models constructed using other methods, finding that our model revealed far more precise structural information on the dural

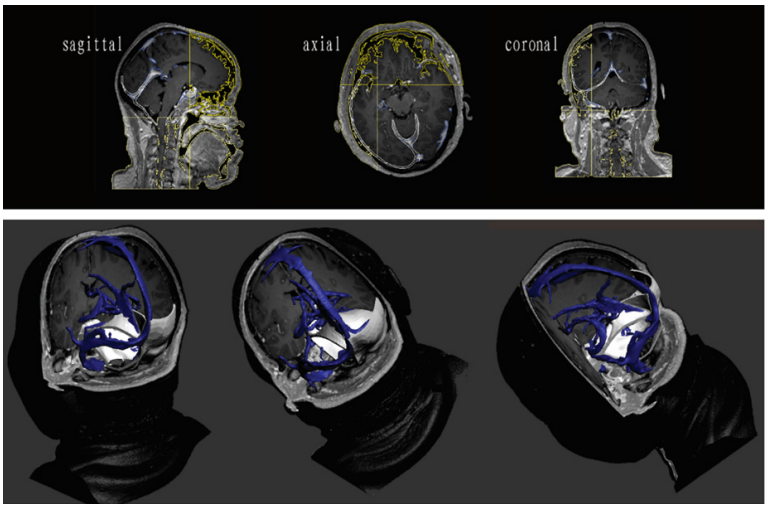

Figure 7. The consistency of dural sinus and deep vein atlas with the corresponding parts in reference model

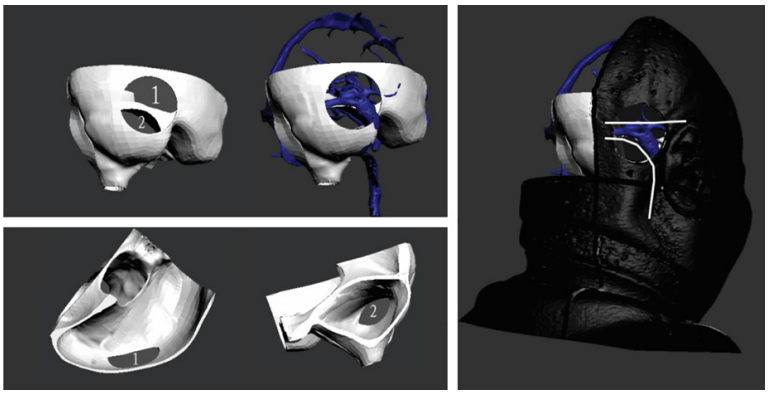

Figure 8. An example demonstration of the assistance of our 3D atlas for a preoperative precise surgical approach planning.

sinuses (**Figure 9**). The model of the venous sinuses and deep veins in PDF format can be rotated 360 degrees in any plane using any structure as the focus of rotation (**Figure 10**).

An additional human dural sinus atlas obtained by using similar materials and the same method is shown in Supplementary Figure 1.

Discussion

Understanding anatomical structures is of fundamental importance for neurosurgeons and an interactive and intuitive atlas provides a readily understandable and maneuverable tool for neuroanatomists and neurosurgeons. In this study, by using a novel approach, we constructed a 3D digital atlas of the dural sinuses and deep veins using contrast-enhanced head MRI data and showed that the atlas can be readily queried by users interactively and lend itself for use in surgical training and preoperative planning. Compared to traditional atlases, our digital atlas has several important advantages. First and foremost, the 3D digital atlas allows us to study the anatomy of the dural sinus and deep veins from any possible angle, eliminating the limitations viewing from an inherently restricted angle of 2D atlases. Second, the 3D digital atlas not only allows users to identify the relative position of the dural sinus and deep veins, but also allows them to better appreciate the actual shape of the dural sinus and deep veins. Third, the atlas can be freely manipulated and dissected. Last, because our atlas was generated from reconstructed head MRI images, the shape of the venous sinus and deep veins more closely mimics the in-vivo scenarios compared to 2D atlases which are based on histological sections.

Atlases not only have great value in medical teaching, but also provide valuable information, particularly in diagnosing diseases and guiding therapies for clinicians. Early atlases consist of autopsy photographs and manual drawings of histological sections, and lack 3D information and are not interactive. Digital atlas is characterized by digitalization and visualization of anatomical information [12] and offers an interactive tool for users. Though numerous digital atlases are available of the brain, cerebrovascular, skull based and cranial nerves [13-17], few atlases of the dural sinus have been published. Our digital atlas is well suited to the task of selecting an appropriate surgical approach that can avoid injuries to specified regions. It also facilitates preoperative planning, as in the case of resecting a posterior fossa tumor, the atlas could be employed to calculate the position of the flap and bone window.

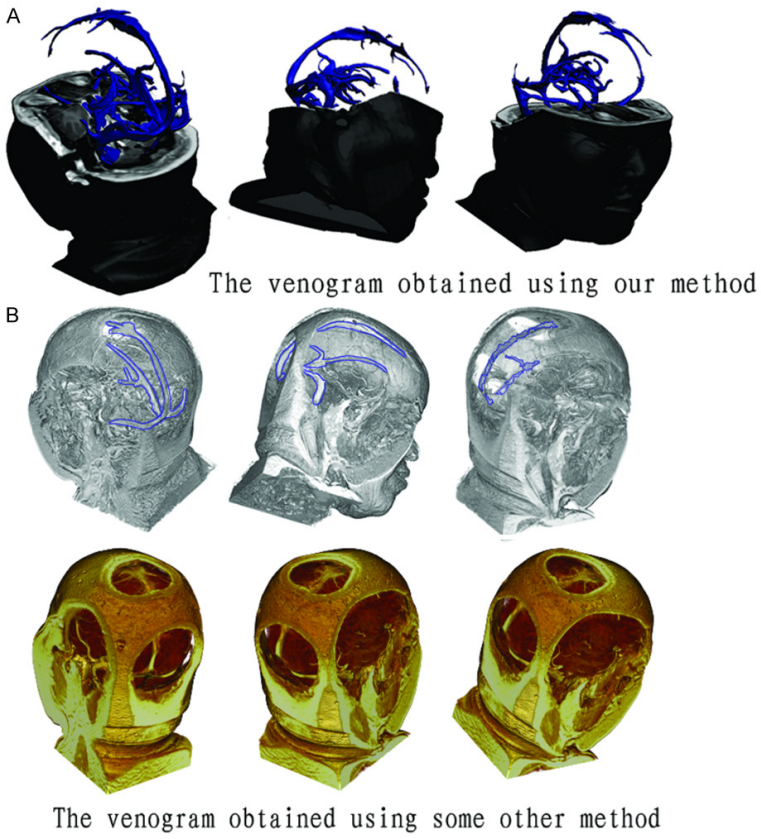

Figure 9. The comparison of dural sinus atlas constructed by different methods.

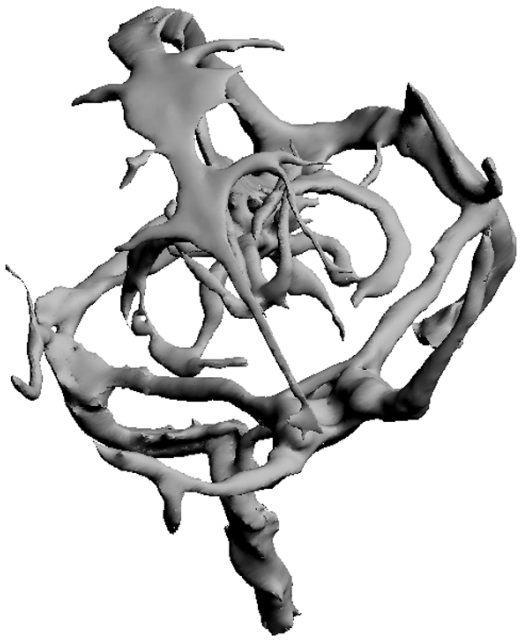

Figure 10. PDF's file of the dural sinus and deep veins. The model can be rotated 360 degrees in any plane using any structure as the focus of rotation.

In 3D model reconstruction, segmentation of target images is based on the gray contrast or boundaries of different tissues. However, segmentation of some structure is not successful, particularly when the gray contrast between target tissue and the surrounding in the original image is too low. The dural sinus wall is very thin and its density is very close to the surrounding tissues, and its boundary is not clear. Consequently, it is very challenging to segment the dural sinus by just using a single method. In the current study, we developed a comprehensive modeling protocol consisting of five steps including thresholding, crop mask, region growing, 3D calculating and 3D editing. The protocol has successfully yielded an accurate and smooth surface model of the venous sinus and deep veins. An atlas is required to be of very high accuracy, and our method has proven to work well even for images with rather poor quality. The current method is semi-automatic: the noise of the rough cast from 3D calculating can be deleted manually by 3D edit in the 3ds-Max and noises can be filtered out after careful screening.

Accuracy of digital atlas is a key issue. We evaluated the atlas accuracy in several ways. On the one hand, we evaluated the accuracy of our 3D atlas by cross-sectioning the surface models with the original head MR image. On the other hand, we evaluated consistency between the marker point and its corresponding coordinates in the three orthogonal slices. The model contours match very well on the venous sinus and deep venous walls of raw head MRI images in three orthogonal (axial, coronal and sagittal view) MRI cross-sections. By clicking a point in the 3D model, the three orthogonal slices comprising this point will display, and the corresponding coordinates will be automatically adjusted. The atlas can be made into a small

movie to play or can be installed on the PC for viewing. The atlas can be arbitrarily zoomed, rotated and cut according to the needs of the observers. Moreover, the atlas can be displayed in a computer in the operating room for intraoperative observation, while printed atlases are not convenient for such purposes. However, no matter how elegant the 3D atlas obtained from head MRI is, it may be still not sufficient for presenting the full anatomic detail of the venous sinuses and deep veins and we believe that our 3D digital atlas could be further improved in the future with advancement of imaging and computing technologies.

Conclusion

An orderly synthesis method for building a 3D digital atlas of the dural sinus and deep veins was developed. The accuracy of the atlas was proved to be sufficient for the purpose of medical education, and guidance for surgical operation.

Disclosure of conflict of interest

None.

Address correspondence to: Drs. Zhirong Yang and Zhilin Guo, Department of Neurosurgical, The Ninth People Hospital, Medical School, Shanghai Jiaotong University, 639 Zhizaoju Road, Shanghai 200011, China. Tel: +86 021-23271699-5155; E-mail: zhirongy@sina.cn (ZRY); gzlysr@126.com (ZLG)

References

[1] Browder J, Browder A, Kaplan HA. Anatomical relationships of the cerebral and dural venous systems in the parasagittal area. Anat Rec 1973; 176: 329-32.

[2] Bonnal J, Brotchi J. Surgery of the superior sagittal sinus in parasagittal meningiomas. J Neurosurg 1978; 48: 935-45.

[3] Giombini S, Solero CL, Lasio G, Morello G. Immediate and late outcome of operations for Parasagittal and falx meningiomas. Report of 342 cases. Surg Neurol 1984; 21: 427-35.

[4] Ransohoff J. Removal of convexity, parasagittal, and falcine meningiomas. Neurosurg Clin N Am 1994; 5: 293-7.

[5] Kondziolka D, Flickinger JC, Perez B. Judicious resection and/or radiosurgery for parasagittal meningiomas: outcomes from a multicenter review. Gamma Knife Meningioma Study Group. Neurosurgery 1998; 43: 405-13; discussion 13-4.

[6] DiMeco F, Li KW, Casali C, Ciceri E, Giombini S, Filippini G, Broggi G, Solero CL. Meningiomas invading the superior sagittal sinus: surgical experience in 108 cases. Neurosurgery 2004; 55: 1263-72; discussion 72-4.

[7] Bassiouni H, Hunold A, Asgari S, Stolke D. Tentorial meningiomas: clinical results in 81 patients treated microsurgically. Neurosurgery 2004; 55: 108-16; discussion 16-8.

[8] Gabibov G KA, Kozlov A, Korshanov A,Timirgaz V, Kalinina E. Surgical results and prognostic factors in parasagittal meningiomas. Experience in 1546 operations. Abstract, 10th European Congress of Neurosurgery 1995, Berlin; May 7-12.

[9] H O. The surgical treatment of intracranial tumors. Handbuch der Neurochirurgie 1967; 4: 1-191.

[10] Kemp WJ 3rd, Tubbs RS, Cohen-Gadol AA. The innervation of the cranial dura mater: neurosurgical case correlates and a review of the literature. World Neurosurg 2012; 78: 505-10.

[11] Yang Z, Guo Z. A three-dimensional digital atlas of the dura mater based on human head MRI. Brain Res 2015; 1602: 160-7.

[12] Toga AW, Thompson PM, Sowell ER. Mapping brain maturation. Trends Neurosci 2006; 29: 148-59.

[13] Haber SN, Calzavara R. The cortico-basal ganglia integrative network: the role of the thalamus. Brain Res Bull 2009; 78: 69-74.

[14] Saikali S, Meurice P, Sauleau P, Eliat PA, Bellaud P, Randuineau G, Vérin M, Malbert CH. A three-dimensional digital segmented and deformable brain atlas of the domestic pig. J Neurosci Methods 2010; 192: 102-9.

[15] Ganser KA, Dickhaus H, Metzner R, Wirtz CR. A deformable digital brain atlas system according to Talairach and Tournoux. Med Image Anal 2004; 8: 3-22.

[16] Calzavara R, Mailly P, Haber SN. Relationship between the corticostriatal terminals from areas 9 and 46, and those from area 8A, dorsal and rostral premotor cortex and area 24c: an anatomical substrate for cognition to action. Eur J Neurosci 2007; 26: 2005-24.

[17] Haber SN, Kim KS, Mailly P, Calzavara R. Reward-related cortical inputs define a large striatal region in primates that interface with associative cortical connections, providing a substrate for incentive-based learning. J Neurosci 2006; 26: 8368-76.

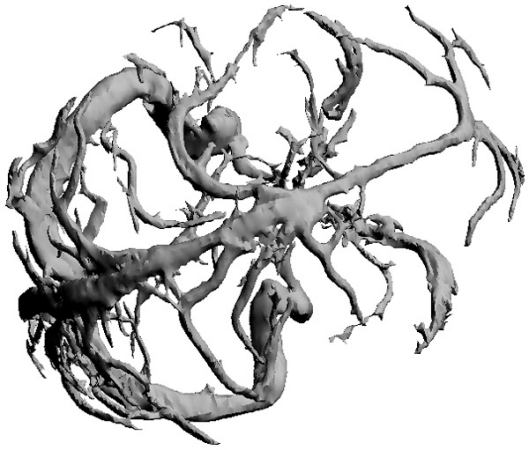

Supplementary Figure 1. PDF's file of the dural sinus and deep veins of the second example constructed with the same method.